Title

Unraveling Metabolic and Proteomic Features in Soybean Plants in Response to Copper Hydroxide Nanowires Compared to a Commercial Fertilizer

Journal

Environmental Science and Technology, 55(20)

ISSN

0013-936X

Authors

Majumdar, Sanghamitra
Long, Randall W
Kirkwood, Jay S
et al.

Publication Date

2021-10-19

DOI

10.1021/acs.est.1c00839

Peer reviewed

Environmental Science & Technology

pubs.acs.org/est

Article

Unraveling Metabolic and Proteomic Features in Soybean Plants in Response to Copper Hydroxide Nanowires Compared to a Commercial Fertilizer

Sanghamitra Majumdar, Randall W. Long, Jay S. Kirkwood, Anastasiia S. Minakova, and Arturo A. Keller*

Cite This: https://doi.org/10.1021/acs.est.1c00839

Read Online

ACCESS | Metrics & More | Article Recommendations | Supporting Information

ABSTRACT: Mechanistic understanding of the interaction of copper-based nanomaterials with crops is crucial for exploring their application in precision agriculture and their implications on plant health. We investigated the biological response of soybean (*Glycine max*) plants to the foliar application of copper hydroxide nanowires (CNWs) at realistic exposure concentrations. A commercial copper based-fungicide (Kocide), dissolved copper ions, and untreated controls were used for comparison to identify unique features at physiological, cellular, and molecular levels. After 32 d of exposure to CNW (0.36, 1.8, and 9 mg CNW/plant), the newly developed tissues accumulated significantly high levels of Cu (18−60 μg/g) compared to Kocide (10 μg/g); however, the rate of Cu translocation from the site of CNW treatment to other tissues was slower compared to other Cu treatments. Like Kocide, CNW exposure at medium and high doses altered Co, Mn, Zn, and Fe accumulation in the tissues and enhanced photosynthetic activities. The proteomic and metabolomic analyses of leaves from CNW-treated soybean plants suggest a dose-dependent response, resulting in the activation of major biological processes, including photosynthesis, energy production, fatty acid metabolism, lignin biosynthesis, and carbohydrate metabolism. In contrast to CNW treatments, Kocide exposure resulted in increased oxidative stress response and amino acid metabolism activation.

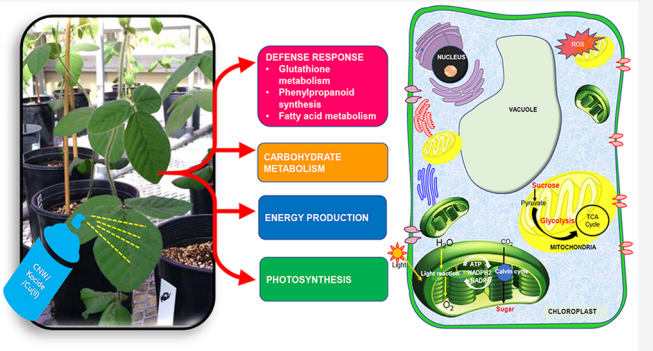

KEYWORDS: *copper hydroxide nanowires, Kocide, soybean, proteomics, metabolomics, gas exchange, lignin*

INTRODUCTION

Nanotechnology has evidently become a promising tool in precision agriculture that provides opportunities to utilize resources in a more efficient and strategic manner with reduced environmental impact and costs.[1] There has been a steady increase in the development of novel agrochemical products employing nanomaterials by adapting traditional ones to enhance their effectiveness, absorption, and controlled release to regions of interest in crops. However, this also brings significant regulatory challenges due to the limited understanding of their mechanism of action and long-term impact on the environment and human health. The U.S. Environmental Protection Agency regulates the use of nanomaterials in pesticide products under the Federal Insecticide, Fungicide, and Rodenticide Act (FIFRA) and is responsible for determining their efficacy, safety, and conditions that can limit or eliminate any potential risks.[2] However, there is a substantial need to adopt modern hazard evaluation and risk-assessment protocols and utilize high-throughput methods to determine the mechanism of action of novel nanomaterials and understand their benefits and potential unintended effects.[3]

Copper is an essential nutrient that is critical to plant metabolic processes including photosynthesis, electron transport, respiration, oxidative stress response, hormone signaling, cell wall metabolism, transcription signaling, protein trafficking, oxidative phosphorylation, and iron mobilization.[4] It also acts as a cofactor in metalloproteins such as cytochrome-*c* oxidase in mitochondria, plastocyanin and polyphenol oxidase in chloroplast, extracellular laccases, and Cu/Zn superoxide dismutase (SOD) in cytosol and chloroplast.[5] However, at high concentrations, redox cycling between Cu oxidation states can catalyze the production of hydroxyl radicals, which can damage biomolecules.[6] Copper is used in numerous registered agrochemicals, in the form of copper sulfate pentahydrate, basic copper sulfate, copper hydroxide, cuprous oxide, copper

Special Issue: Environmental Implications of Nanofertilizers

Received: February 11, 2021
Revised: June 8, 2021
Accepted: June 23, 2021

oxychloride, copper ammonium carbonate, and copper octanoate.[7] The ability of Cu ions to bind to functional groups of proteins to cause protein denaturation and cell damage is leveraged in crop protection. Some commercial pesticides such as CuPro and Kocide-3000 DuPont (Kocide) are constituted of $Cu(OH)_2$ nanosheets; however, given the micron-scale size of the final material, these pesticides are not regulated as "*nanopesticides*".[8] The effects of nanoscale Cu-based formulations have been shown to vary across crop species depending on the particle properties, mode of application, and growth conditions.[9−16] Metabolomic studies in lettuce, cucumber, corn, and maize show implications for energy metabolism and plant defense systems.[11,17,18] Recent studies have shown that CuO nanoparticles (*n*CuO), $Cu_3(PO_4)_2$ nanosheets, and CuO nanosheets enhance nutrient acquisition and bolster innate defense system in plants by the transcription of defense and health related genes.[19−21] Although the effects of Kocide have been studied widely in crops at physiological and metabolic levels, the underlying mechanisms at the protein level are unexplored. In addition, there is limited information on the interaction of crops with nanoscale $Cu(OH)_2$ particles, which show potential agronomic benefits comparable to Kocide.[22] Soybean (*Glycine max*) is a globally important legume crop that is a major source of proteins and fatty acids and is a good candidate to study discovery proteomics and metabolomics due to incrementing data availability on the functional annotation of soybean genes.[23]

The current study evaluates the hypotheses that soybean plants will demonstrate increased photosynthetic potential in response to $Cu(OH)_2$ nanowires (CNWs) compared to untreated controls, and the underlying mechanism aided by the responsive proteins and metabolites will be distinct from Kocide and dissolved Cu(II)-ion exposures. We investigate the effect of the foliar application of CNWs at realistic exposure concentrations on nutrient accumulation, lignification, and photosynthesis in soybean plants during vegetative and flowering stages under greenhouse conditions. These end points were compared with untreated controls, micron-sized Kocide and dissolved Cu(II)-ion exposures. Liquid chromatography−tandem mass spectrometry (LC−MS/MS)-based proteomic and metabolomic analyses of leaves were used to identify the biomarkers of exposure unique to CNWs treatments.

MATERIALS AND METHODS

Chemicals. CNWs (50 nm diameter, 3−5 μm long, 99.5% pure, 65% Cu) were procured from US Research Nanomaterials Inc. As per the manufacturer's report, these particles were produced by calcination and precipitation without the addition of any stabilizer. For a comparative exposure assessment, we used a commercial $Cu(OH)_2$-based fungicide product, Kocide-3000 DuPont (26.5% Cu), and $CuSO_4{\cdot}5H_2O$ (25.4% Cu, referred as $CuSO_4$).

Plant Growth Conditions. Soybean (*Glycine max* L. var. Envy) seeds purchased from Seed Savers Exchange (Decorah, IA) were surface sterilized with 2% sodium hypochlorite solution and rinsed thoroughly and soaked in nanopure water (NPW, 18.2 MΩ·cm at 25 °C) for 1 h. The seeds were germinated in seed-starter trays and then grown in small pots (10.2 cm × 7.6 cm; three seedlings/pot) for 22 days. Upon the appearance of the first true leaf, each healthy and uniform-sized seedling was transplanted to individual pots (20.5 cm × 21.6 cm) and used for exposure assay after 2 days. An artificial soil mixture composed of sand (Quikrete Washed Plaster Sand), organic potting-mix, vermiculite (Therm-O-Rock), coco coir (Canna), and perlite (Therm-O-Rock), at a ratio of 1:1:2:3:4 by volume, was used for germination and plant growth. The soil mixture was amended with 0.4% (v/v) 4-4-4 NPK-fertilizer. Plants were grown in greenhouse conditions, maintained at 25 ± 3 °C and a 14 h photoperiod throughout the experiment. Plants were irrigated every alternate day with NPW.

Foliar Spray Exposure Experiment. For foliar exposure, 24 day old soybean plants were sprayed with aqueous colloidal suspensions of CNWs or Kocide, $CuSO_4$ solution, or NPW, using a commercial hand-held sprayer. The doses were selected on the basis of the manufacturer's recommendation for the field application of Kocide on soybean plants (0.84−1.68 kg/ha ≈ 2.2−4.5 mg/plant). The higher application rate was selected for the exposure studies, which represents 1.2 mg Cu/plant. Three different treatment levels were selected for CNWs (CNW-L, 0.36 mg CNW/plant; CNW-M, 1.8 mg CNW/plant; CNW-H, 9 mg CNW/plant, contributing 0.24, 1.2, and 6 mg Cu/plant, respectively). Preliminary dissolution studies using Amicon 3KDa centrifugal filters suggested a ≤10% dissolution of Cu(II)-ions from CNW suspensions. Thus, to evaluate the effect of dissolved Cu(II)-ions, $CuSO_4$ exposure with a dose equivalent to 10% CNW-M was chosen (0.48 mg $CuSO_4$/plant).

Foliar spray was optimized for delivering and reporting accurate exposure doses. Preliminary experiments suggested that only 10% of spray volume from the hand-held sprayer is retained by the soybean foliage (∼0.001 L). To supply the requisite amount of Cu from the different treatments in a total volume of 6 mL, 80 mg/L $CuSO_4$, 755 mg/L Kocide, and 60, 300, and 1500 mg/L CNW treatments were prepared fresh on the day of exposure. CNW and Kocide treatments were prepared by sonicating 0.05 L of each suspension for 5 min using a sonication probe fitted with a microtip (S-4000, Misonix Ultrasonic, Farmingdale, NY) at 40% amplitude (input power 7 W) (Supporting Information (SI), Figure S1). To avoid overheating, a pulsed sonication for 2 s was adopted and the tubes were kept in a secondary container with ice water. The suspensions were diluted 4 times with NPW, followed by a 15 min bath sonication (Branson 8800, Danbury, CT). The average hydrodynamic diameter and ζ-potential of the suspended CNW and Kocide particles were measured immediately after bath sonication using a Zetasizer Nano-ZS (Malvern Instruments, Worcestershire, UK) at 25 °C. The stability of the suspensions was tested after 0, 24, 48, and 96 h of preparation.

Plants were sprayed in six separate spray events over 2 days, under shade without any direct artificial or natural lighting. Each day, the plants were sprayed three times, with a 1 h interval between each event to allow the droplets to dry. The plants were weighed before and after each spraying event to report the exact dose. The average cumulative mass of the suspensions retained on the aerial tissues after six spray events across all the treatments was recorded as 6.1 ± 0.1 g. The soil was covered with a customized plastic cover to avoid contamination from the spray or dripping of excess droplets from the leaves (Figure S1). The experiment was conducted in two staggered sets, each used for different experimental goals. Each set consisted of four replicates per treatment, including an "untreated control" where NPW was sprayed to the foliage. The pots were randomly arranged on the greenhouse bench and rearranged twice a week.

Physiological Parameters and Element Content. The first set of soybean plants was used to record physiological and gas exchange parameters periodically, and the plants were harvested after 16 and 32 d of exposure to determine elemental

https://doi.org/10.1021/acs.est.1c00839
Environ. Sci. Technol. XXXX, XXX, XXX−XXX

content in the tissues. The roots were washed under tap water to discard the adhered soil particles, followed by rinsing the plant three times alternately with 0.1% (v/v) HNO_3 and NPW. To test the extent of adsorption and absorption of various treatments on the aerial tissues, two separate sets of three plants were analyzed for total Cu content after 1 d of exposure, with and without rinsing the shoots. Shoot and root lengths were measured to evaluate the effects on plant growth and overt plant health in response to different Cu treatments. The wet plants were dried at 25 °C for 1 h, roots and stems were separated, and fresh biomass was recorded across all the treatments.

Roots and shoots were dried at 70 °C for 96 h, weighed, and digested using 1:4 (v/v) HNO_3/H_2O_2 heated at 115 °C for 40 min on a heat block (DigiPREP System; SCP Science). The digested contents were diluted to fit the calibration curve prepared using multielemental standards. A standard reference material (spinach leaves, NIST 1570A) was processed with every batch of samples, and ≥95% recovery was achieved for all the elements. The digested tissues were analyzed for Cu, Co, Fe, Mn, Mo, Ni, Zn, Ca, K, Mg, Na, and P using inductively coupled plasma mass spectrometry (Agilent ICP-MS 7500, Agilent Technologies, Santa Clara, CA). Analytical and matrix blanks were analyzed, and a calibration verification standard was run every 12 samples.

Gas Exchange Measurements. Spot gas exchange surveys were performed on 5, 12, and 21 d after foliar exposure, using a portable infrared gas analyzer (LI-6400xt, LI-COR, Lincoln, NE) equipped with a 2×3 cm^2 leaf chamber and a red/blue light source (6400-02B, LI-COR), as described in detail in SI Method S1. Briefly, the measurements were made by selecting the most recent fully expanded leaf, typically the second or third one from the apical meristem, and allowing the leaf to adapt to the chamber for approximately 2 min. Three measurements were averaged to obtain net photosynthesis (A_{net}; assimilated CO_2 $\mu mol \cdot m^{-2} \cdot s^{-1}$), stomatal conductance (G_s; H_2O $mmol \cdot m^{-2} \cdot s^{-1}$), and transpiration rates (E; H_2O $mmol \cdot m^{-2} \cdot s^{-1}$). Instantaneous water use efficiency (WUE_i) was calculated from A_{net} and E ($WUE_i = A_{net}/E$).

Lignin Quantitation. The second set of plants were harvested after 32 d and washed in NPW. The second fully expanded leaves from the apical meristem across all the treatments ($n = 4$) were severed and individually ground into a fine powder in liquid nitrogen using a set of mortar and pestle, which was rinsed with ethanol between samples. The ground leaf tissues were stored at −80 °C for lignin quantitation and proteomic and metabolomic analyses.

Lignin was determined in the leaves using the acetyl bromide method.[24] Briefly, 0.3 g of ground tissue was freeze-dried (FreeZone 6 L, −50 °C; Labconco). Protein-free cell wall pellets obtained from the ground tissues were digested in 25% acetyl bromide, neutralized with 2 mol/L NaOH, and, subsequently, solubilized in freshly prepared 5 mol/L hydroxylamine-HCl solution. The samples were allowed to settle overnight, and the absorbance was measured at 280 nm.

Statistical Analysis. The data acquired for physiological parameters, gas exchange activities, lignin quantification and elemental contents were reported as mean± standard error (SE). A one-way ANOVA was performed followed by Tukey's multiple comparisons test (Origin 2018, Northampton, MA) at $p \leq 0.05$.

Proteomic Analysis. *LC−MS/MS Analysis of Peptides.* Proteins in the frozen ground leaves of each treatment group were extracted following a method by Majumdar et al.[25] After trypsin digestion (1:20), the samples were desalted using a 3M-Empore-C18 extraction disk cartridge and analyzed using a Thermo Scientific UltiMate 3000 RSLCnano system coupled to a Thermo Scientific Q-Exactive-plus Orbitrap mass spectrometer.[26,27] The raw proteomics data were deposited in the ProteomeXchange Consortium *via* the PRIDE partner repository with the data set identifier PXD026456.[28]

The detailed method for protein identification, quantification, and statistical analysis is provided in SI Method S2. In summary, a relative label-free quantification (LFQ) of the acquired data was performed using MaxQuant software (*v*.1.6.17.0) on the basis of the intensity of peptides identified in a full m/z scan. The MS/MS spectra were searched against the *G. max* UniProtKB database (85 051 entries; January 2021) using the Andromeda search engine, and the peptide spectrum match and protein false discovery rate (FDR) were filtered at 1%.[27,29] Protein abundance in the leaves was calculated on the basis of spectral intensities (LFQ intensity) of the matched peptides normalized across all the treatments.

Data Processing. Four separate analyses for feature detection and protein identification/quantification were performed with different subsets, (1) all treatment groups, (2) control and CNWs, (3) CNWs and Kocide, and (4) control and $CuSO_4$, to identify treatment specific proteins. Further processing of the quantitative data obtained on protein groups identified in soybean leaves across three independent biological replicates per treatment was performed using Perseus software (*v*.1.6.15.0), as described in SI Method S2.[30] The proteins were validated across the treatments, and respective LFQ intensities were subjected to analysis of variance (ANOVA) controlled by $p \leq 0.05$ to identify the significant proteins and clustered into groups by hierarchical clustering analysis based on Pearson's correlation. The functional annotation and gene ontology (GO) of the identified proteins were performed using UniprotKB and KEGG tools.[31,32]

Metabolomic Analysis. *LC−MS/MS Analysis of Metabolites.* For an initial screening of the metabolites of interest, untargeted and targeted metabolomic analyses were performed on the leaves from plants exposed to CNW-H, Kocide, $CuSO_4$, and the control, in $n = 3$, as described in SI Method S3. Briefly, finely ground tissues were extracted in a solvent mixture by vortex mixing for 90 min at 4 °C. The extracted samples were centrifuged at 16 000*g* for 15 min at 4 °C, and the supernatants were subjected to an untargeted analysis of nonpolar metabolites and targeted analysis of polar metabolites. The nonpolar fraction of the supernatants was analyzed on a Waters Synapt G2-Si quadrupole time-of-flight mass spectrometer coupled to an I-class UPLC system (SI Method S3).[33] The MS scan range was 50−1600 m/z with a 100 ms scan time, and MS/MS was acquired in a data-dependent fashion. The targeted analysis of 184 polar metabolites was performed on a Waters TQ-XS triple-quadrupole mass spectrometer coupled to an I-class UPLC system, and the MS was operated in selected reaction monitoring mode.[34]

To delve deeper into the metabolic pathways, targeted LC−MS/MS analysis of different groups of metabolites was performed in the leaves from plants exposed to CNW-L, CNW-M, CNW-H, Kocide, $CuSO_4$, and the control, each with four biological replicates. Frozen ground leaf tissues (∼100 mg) were extracted in 1 mL of 80% methanol containing 2% formic acid, followed by vortex, sonication, and centrifugation at 20 000*g* at 4 °C for 20 min at each step. The supernatants were used for the detection and quantification of 82 key metabolites

https://doi.org/10.1021/acs.est.1c00839
Environ. Sci. Technol. XXXX, XXX, XXX−XXX

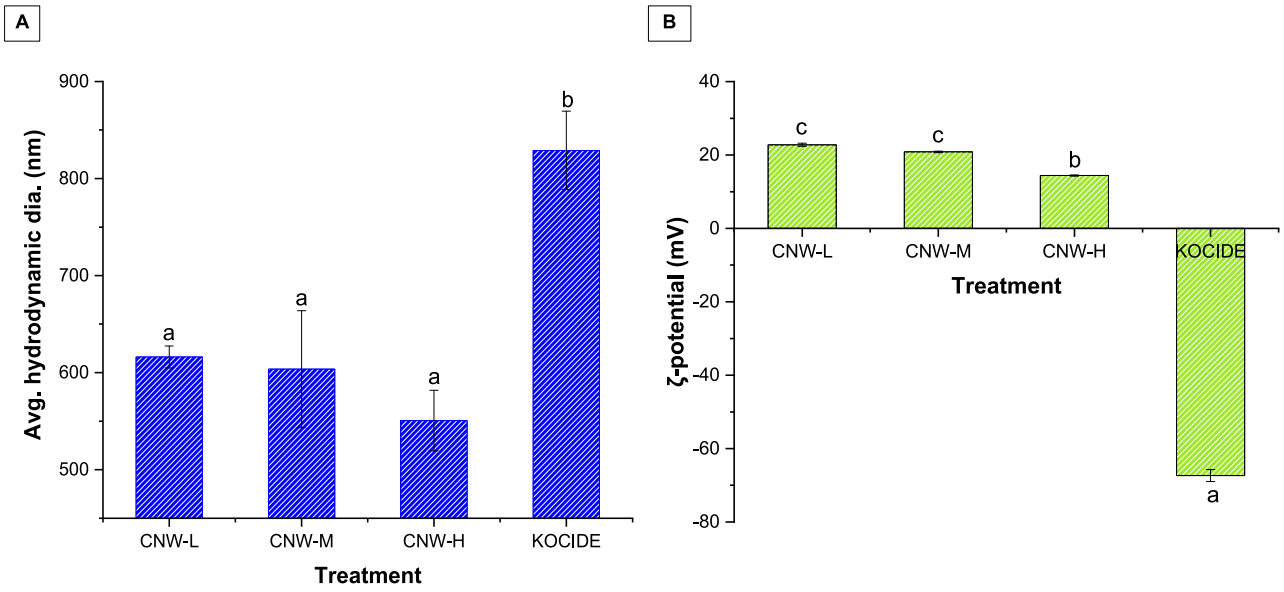

Figure 1. Characteristics of CNWs (CNW-L, CNW-M, and CNW-H) and Kocide in aqueous suspension. (A) Average hydrodynamic diameter (nm) and (B) ζ-potential (mV). Values are expressed as mean ± SE (n = 4). Bars with different letters represent significant differences between the treatments, as determined by one-way ANOVA and Tukey's multiple comparison test ($p \leq 0.05$).

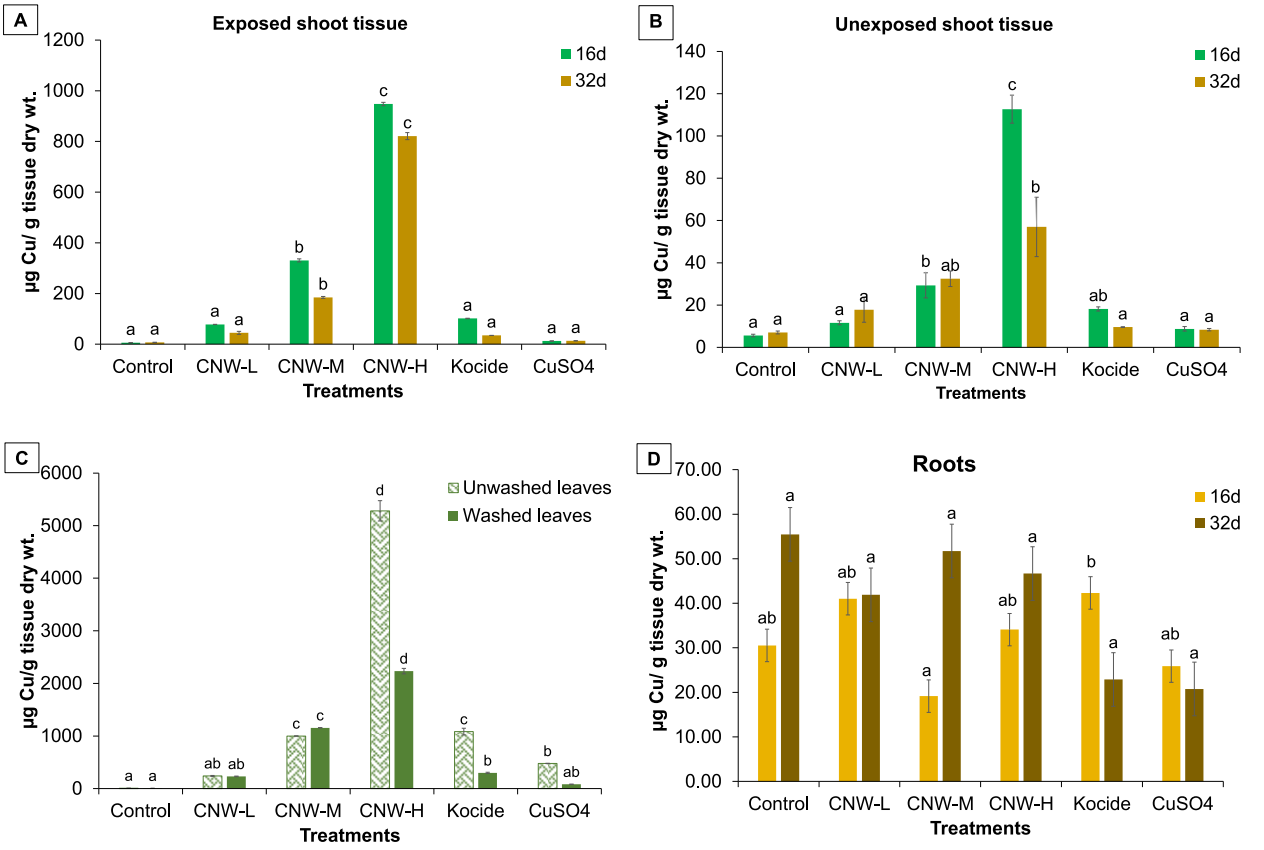

Figure 2. Copper concentration (μg Cu/g tissue dry weight) in plant tissues after foliar exposure to the control, CNW-L, CNW-M, CNW-H, Kocide, and $CuSO_4$ treatments. (A) Exposed shoot tissues after 16 and 32 d. (B) Unexposed shoot tissues after 16 and 32 d. (C) Unwashed and washed exposed leaves after 1 d; (D) Roots after 16 and 32 d. Values are expressed as mean ± SE (n = 4). Bars with different letters represent significant differences between the treatments, as determined by one-way ANOVA and Tukey's multiple comparison test ($p \leq 0.05$).

including amino acids, antioxidants, fatty acids, organic acids/phenolics, nucleobase/side/tides, and sugar/sugar alcohols, with independent methods for each metabolite group using an Agilent 1260 UHPLC binary pump coupled with an Agilent 6470 triple-quadrupole mass spectrometer, as previously described.[27,35,36] The list of metabolites and the information on retention time, parent and product ions, and linearity of the calibration curves are provided in Table S1.

https://doi.org/10.1021/acs.est.1c00839
Environ. Sci. Technol. XXXX, XXX, XXX−XXX

Data Processing. A detailed description of the processing of the acquired untargeted and targeted metabolomics data is provided in SI Method S3. For untargeted metabolomics data, the mass spectral data were processed using Progenesis Qi software (Nonlinear Dynamics).[37−39] An extension of the metabolomics standard initiative guidelines was used to assign an annotation level confidence.[40,41] Data acquired on the Waters TQ-XS MS were processed using Skyline software.[42] The targeted metabolomics data acquired on the Agilent 6470 MS were processed using Agilent MassHunter software (*v*.B.06.00). Statistical analysis of the metabolites was performed using Metaboanalyst 5.0.[43]

Bioinformatics and Pathway Analysis. The differentially accumulated proteins (DAPs) in the soybean exposed to CNWs and Kocide were used for protein−protein interaction (PPI) analysis using STRING database (https://string-db.org; *v*.11.0) with a high-confidence interaction score (≥0.7) and pathway enrichment was performed using a *G. max* database.[44] Metaboanalyst 5.0 was used for pathway enrichment using the metabolites of interest.[43] The common pathways from proteomic and metabolic analysis were merged to investigate the mechanism of interaction.

RESULT AND DISCUSSION

Characterization of CNW and Kocide Suspensions. The aqueous suspensions of copper hydroxide nanowires at three treatment levels (CNW-L, CNW-M, and CNW-H) and Kocide were characterized for particle size and surface charge at 0, 24, 48, and 96 h after sonication. The average hydrodynamic diameters of CNW-L, CNW-M, and CNW-H at 0 h were 616 ± 11, 604 ± 60, and 551 ± 31 nm, respectively (Figure 1A). Although a decreasing trend in hydrodynamic size of the aggregates was noted with increasing CNW concentration, it was statistically insignificant ($p > 0.7$). Kocide particles formed significantly ($p = 0.006$) larger aggregates (829 ± 40 nm) compared to those of CNWs. The ζ-potentials of the CNW-L, CNW-M, CNW-H, and Kocide particles were 22.8 ± 0.4, 20.8 ± 0.2, 14.4 ± 0.2, and −67.3 ± 1.6 mV, respectively. (Figure 1B). In contrast to positively charged CNWs, large stable aggregates and a negative charge of Kocide particles in suspension were attributed to the organic moieties that bound $Cu(OH)_2$ nanosheets in the formulation.[8,45] Sonication was determined as the preferred method for resuspension as vortex mixing was inefficient in resuspending CNWs in water when stored for 96 h (Figure S2). At a high concentration, CNW aggregates rapidly within 24 h and vortex mixing is not enough to resuspend them. However, 15 min of sonication successfully resuspended the CNW in suspension at all concentrations. The organic binder in Kocide enables the particles to remain stable for at least 96 h in aqueous suspension, irrespective of the resuspension method.

Plant Growth, Copper Mobility, and Nutrient Acquisition. Soybean plants did not show any overt symptoms of toxicity in response to CNW or Kocide (Table S2, Figure S3). Although there was an apparent increase in shoot length after 32 and 52 d of exposure to CNW-H and 52 d of exposure to Kocide, the increase was not statistically significant. However, acute exposure to Cu(II)-ions from $CuSO_4$ solutions showed a discoloration of the exposed leaves, which suggests the impairment of chlorophyll to function normally in the photosynthetic process.[46] The negative effect of direct exposure to Cu(II)-ions was reflected in the decreased shoot length of the plants compared to other treatments.

Copper accumulation was determined in soybean roots, aerial tissues exposed to Cu treatments (exposed shoot), and newly formed aerial tissues (unexposed shoot) (Figure 2A−D). The determination of Cu in shoot tissues without surface rinsing confirmed that CNW-M- and Kocide treatments resulted in similar Cu levels (999 ± 2 and 1084 ± 63 μg/g tissue) (Figure 2C). Compared to CNW-M exposure, CNW-L- and CNW-H-exposed shoots yielded around 5 times lower (241 ± 9 μg/g tissue) and 5 times higher (5282 ± 195 μg/g tissue) Cu levels in shoots, respectively, thereby validating the spraying process. To test Cu absorption by the leaves after 24 h of exposure, shoots were surface rinsed to remove adhering Cu particles on the leaf surface. CNW-L and CNW-M treatments showed >95% retention of Cu in shoot tissues; however, CNW-H and Kocide treatments showed 42% and 27% retention, respectively. This suggests increased bioavailability and less wash-off of CNWs compared to Kocide and hence better resource utilization.

After 16 d of exposure to CNW-L, CNW-M, CNW-H, Kocide, and $CuSO_4$, the exposed shoot tissues accumulated 78, 331, 948, 102, and 12.7 μg Cu/g tissue, respectively, and the unexposed tissues accumulated 12, 29, 113, 18, and 9 μg Cu/g tissue, respectively (Figure 2A). Similarly, after 32 d of exposure to a similar Cu dose (1.2 mg/plant), CNW-M showed an increased Cu accumulation in the unexposed tissues (32 μg/g) compared to Kocide treatment (10 μg/g) (Figure 2B). After 32 d of exposure, the Cu content in the shoot tissues of CNW-M- and CNW-H-treated plants decreased compared to that of 16 d; however, a simultaneous increase in root Cu content in the 32 d treatments was observed with respect to 16 d (Figure 2D). The translocation factors were calculated as $[Cu]_{\text{unexposed shoot}}/[Cu]_{\text{exposed shoot}}$ and $[Cu]_{\text{root}}/[Cu]_{\text{exposed shoot}}$. The aerial translocation factor of Cu in soybean plants after 16 d of exposure was in the order of $CuSO_4$ > Kocide > CNW-L > CNW-H > CNW-M; however, after 32 d, CNW-L showed a higher aerial translocation than Kocide (Table S3). Copper translocation to the roots was also highest in $CuSO_4$, followed by CNW-L, Kocide, CNW-M, and CNW-H. Kocide and $CuSO_4$ treatments resulted in low Cu accumulation in shoots compared to CNW-M treatments after 16 d, which could be attributed to two factors: (1) lower Cu absorption by the leaf tissues (Figure 2C) and (2) a higher rate of translocation to newer unexposed tissues and roots (Table S3) in Kocide and $CuSO_4$ treatments, which may also result in exudation *via* roots to avoid toxicity. This also suggests a slow release and translocation of Cu from the applied CNWs compared to Kocide and ionic treatments at similar or higher doses. A higher aerial translocation and limited translocation to roots of Cu from nanoscale Cu compounds have also been previously reported, demonstrating an increased xylem transport of Cu.[10,17,21,47] Our study however suggests that CNW foliar exposure may not be the best choice if the application demands translocation to the roots.[21]

Although CNW-L-exposed shoots accumulated significantly less Cu than CNW-M and CNW-H, it accumulated significantly more Zn than other Cu treatments after 16 d of exposure (Table S4). $CuSO_4$ exposure resulted in a decrease in Co levels in the unexposed shoots compared to CNW-H and Kocide, and an increase in Fe levels than the control treatments. However, 16 d of CNW exposure exhibited a dose-dependent response on K, Co, Fe, and Mn accumulation in the roots. Roots from 16 d CNW-L exposure accumulated significantly higher levels of K, Co, and Mn compared to those of CNW-M and CNW-H; whereas CNW-H roots accumulated high levels of Fe compared to all Cu treatments. The high Cu content in CNW-H shoots

https://doi.org/10.1021/acs.est.1c00839
Environ. Sci. Technol. XXXX, XXX, XXX−XXX

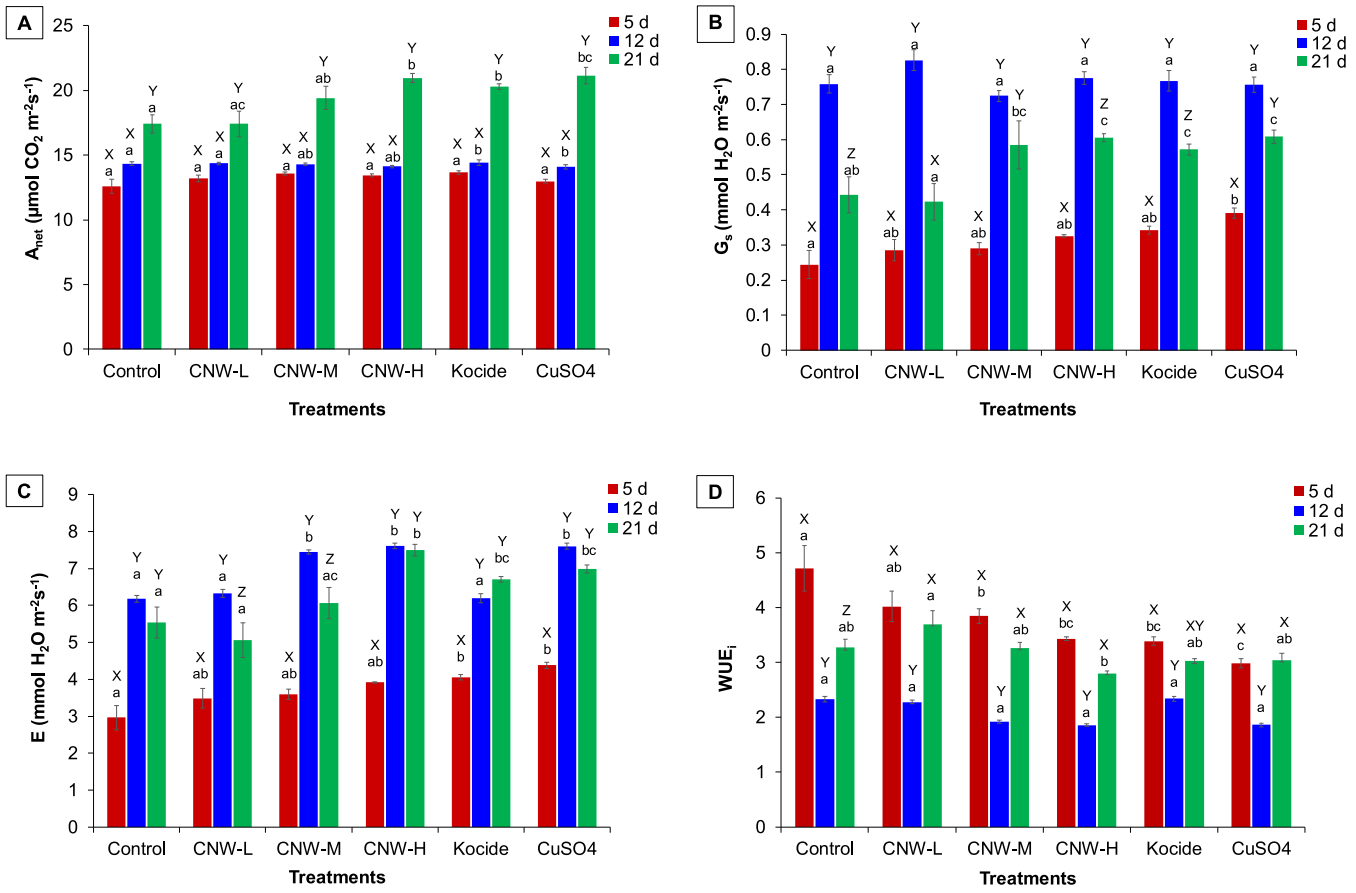

Figure 3. Gas exchange activities in soybean plants. (A) Net photosynthesis rate, A_{net} (μmol CO_2 $m^{-2}\cdot s^{-1}$). (B) Stomatal conductance rate, G_s (mmol H_2O $m^{-2}\cdot s^{-1}$). (C) Transpiration rate, E (mmol H_2O $m^{-2}\cdot s^{-1}$). (D) Water use efficiency, WUE_i (A_{net}/E) in the most recent fully expanded leaf after 5, 12, and 21 d of foliar exposure to the control, CNW-L, CNW-M, CNW-H, Kocide, and $CuSO_4$ treatments. Values are expressed as mean ± SE ($n = 4$). Bars with different letters represent significant difference between the treatments (a, b, c) and between days of exposure within a treatment (X, Y, Z), as determined by one-way ANOVA and Tukey's multiple comparison test ($p \leq 0.05$).

may activate redox-cycling between Fe and Cu and chelation of the metal to ligands, metallochaperones, or storage proteins.[5] This may also affect the photosynthetic electron transport, which is heavily dependent on Fe- and Cu-associated proteins in the chloroplast.[5] Cu, Zn, Fe, and Mn are redox-active metals that participate as cofactors in Cu/Zn-SODs, Fe-SODs, and Mn-SODs as the first line of defense against reactive oxygen species (ROS). The simultaneous dysregulation in Cu, Fe, Mn, and Zn levels in CNW-L indicate probable activation of SODs at low exposure doses. In 32 d exposed shoot tissues, the Cu treatments did not interfere with nutrient acquisition (Table S5). However, the roots from $CuSO_4$ exposure showed depleted levels Co, Fe, Mn, and Zn. This could be a defense strategy by the $CuSO_4$-treated plants to restrict micronutrient uptake in response to rapid Cu translocation to the unexposed tissues, thereby resulting in stunted aerial growth in these plants (Figure S3).

Lignification and Gas Exchange Activities. Lignin is a complex and branched polymer of phenolic compounds, which is the final product of the phenylpropanoid pathway in plants and plays a crucial role in the defense response of plants. After 16 d of exposure, only CNW-M treatment showed significantly high lignin accumulation (Figure S4). However, the unexposed leaves from CNW-M, CNW-H, and Kocide treatments showed an increasing trend in lignin content, compared to the control treatment. The unexposed and exposed leaves from CNW-L treatment accumulated significantly less lignin than those of CNW-M, CNW-H, and Kocide treatments ($p < 0.05$). After 32 d of exposure, the lignin content in the unexposed leaves of all Cu treatments were similar to that of the control treatment. Studies have suggested that Cu acts as a cofactor in enzymes such as laccase and peroxidase; hence, during the early growth stage, laccase could be responsible for lignin biosynthesis in Cu-treated tissues; and with prolonged incubation period, laccases and peroxidases may work cooperatively in lignin biosynthesis.[48]

Compared to untreated control plants, the net photosynthesis rate was significantly higher in plants exposed to Kocide and $CuSO_4$ after 12 d of exposure; however, after longer exposure for 21 d, A_{net} was significantly higher in all the treatments, except CNW-L and CNW-M (Figure 3A). The $CuSO_4$, CNW-H, Kocide, and CNW-M treatments resulted in 21.3%, 20.3%, 16.6%, and 11.5% increases in A_{net}, respectively. A similar increasing trend was observed in stomatal conductance rates in the plants after 21 d of exposure to CNW-M, CNW-H, Kocide, and $CuSO_4$ (Figure 3B). The transpiration rates were however increased within 5 d of exposure to all the treatments but were only significant for Kocide and $CuSO_4$, compared to the control (Figure 3C). With the increasing period of exposure (12 and 21 d), the transpiration rates were consistently high for all the treatments, except CNW-L. Interestingly, the WUE_i decreased in all the Cu treatments within 5 d of exposure, compared to the control. However, it was restored to normal level in all the Cu-treated plants after 12 d of exposure. (Figure 3D). As observed in

https://doi.org/10.1021/acs.est.1c00839
Environ. Sci. Technol. XXXX, XXX, XXX−XXX

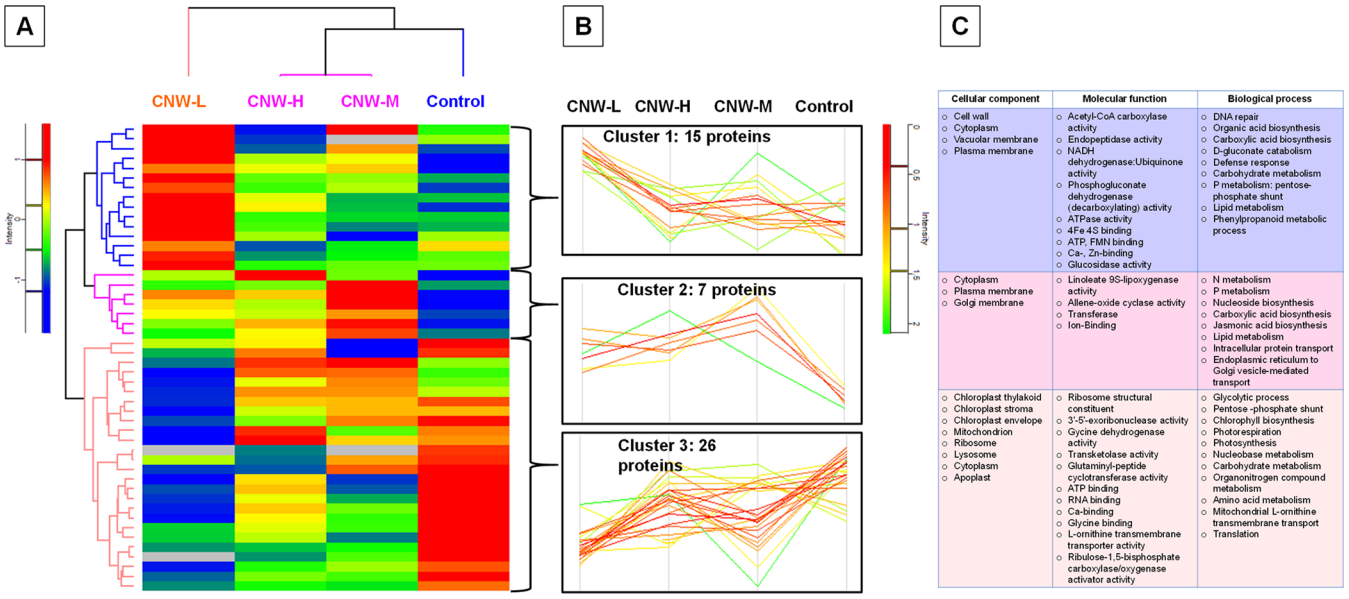

Figure 4. Hierarchical clustering analysis of ANOVA significant leaf proteins after 32 d of foliar exposure to the control, CNW-L, CNW-M, and CNW-H treatments. (A) PLS-DA score plot of metabolites identified. (B) Important features identified by PLS-DA; the colored boxes indicate the relative concentrations of the corresponding metabolite in each group. (C) Hierarchical clustering of the ANOVA significant metabolites (FDR ≤ 0.05); the color bar shows the increase (red) and decrease (green) in the abundance of the metabolites.

the plants after 21 d exposure, high rates of A_{net} may deplete concentrations of CO_2 in the chloroplast and increase mesophyll and stomatal conductance. The trend observed in the gas exchange rates could be attributed to Cu accumulation in the fresh tissues (Figure 2). Since foliar exposures to the Cu treatments were made on older mature leaves that were not used in gas-exchange measurements, the delayed response after 21 d of exposure may be explained by the low mobility of Cu in plant tissues, especially for CNW treatments (Figure 2). CNW-H exposure resulted in the highest Cu accumulation in the newly developed leaves, demonstrating an enhancing effect on the photosynthetic process, which was comparable to Kocide exposure. In a previous study, Cu(II)-ion and *n*CuO exposure administered through soil application negatively affected the gas exchange activities in bell pepper plants grown for 90 days;[49] however, our study demonstrate that the foliar application of Cu improves the overall photosynthetic process in soybeans.

Proteomic Response in Soybean Plants Exposed to CNW. To understand the underlying mechanisms of the physiological response to Cu treatments, proteomic analysis was performed on the leaf samples harvested after 32 d of exposure. A total of 6822 peptides corresponding to 1645 protein groups were identified in the soybean leaves across all the treatments, including the control, CNW-L, CNW-M, CNW-H, Kocide, and $CuSO_4$. Proteins were validated by their presence in at least two replicates of at least one treatment and were considered as *high-confidence proteins* (Table S6). Of the protein groups identified across all the treatments, 19 were common between all Cu treatments and were absent in the untreated control (Figure S5, Table S7). These proteins were predominant in mitochondrial and chloroplast thylakoid membrane and involved in chlorophyll-binding, metal-ion binding, and ATP-binding and transmembrane transport, suggesting the activation of Cu-associated regulatory networks. Some of these proteins were also involved in oxidoreductase activities including shikimate 3-dehydrogenase (NADP+) activity, which plays a critical role in aromatic amino acid biosynthesis (*Phe*, *Tyr*, and *Trp*) through the shikimate pathway.[50] In addition, 18 proteins located in cytoplasm, mitochondria, chloroplast, and peroxisomes were unique to CNW and $CuSO_4$ treatments, which were primarily associated with ATP- and metal-ion-binding and oxidoreductase activity in lignin biosynthetic process and fatty acid β-oxidation (Figure S5). Three unique proteins in CNW and Kocide treatments were associated with ATP-binding and hydrolases involved in proteolysis and amino acid metabolism. Five proteins, viz., pectinesterase, isopentenyl-diposphate δ-isomerase, glycosyltransferase, and glutathione S-transferase, Leuk-A4-hydroC-domain-containing protein, were exclusive to CNW treatments, which were involved in cell wall modification, chlorophyll biosynthesis, flavonoid glycosylation, glutathione metabolism, and Zn-binding, respectively. Compared to the control, all the CNW treatments accumulated 12 proteins, which were located in the mitochondrial proton-transporting ATP-synthase complex, chloroplast thylakoid membrane, nucleus, peroxisomes, and cytosol involved in ion transport, response to oxidative stress, NADP/NADH metabolism, nitrogen metabolic processes, flavonoid and carbohydrate metabolism, photosynthesis, catalytic activity (peroxidase, transferase, lyase, hydrolase), nucleobase-binding, vitamin-binding, and carbohydrate-binding.

Multiscatter analysis was performed to examine the reproducibility of the quantification among the triplicates in each treatment groups. The average Pearson's correlation coefficient of the replicates within each treatment was ≥ 0.95, suggesting a high degree of correlation (Figure S6). The PLS-DA score plot of the identified proteins across all treatments shows that CNW-L and CNW-H treatments were separated from the control, Kocide, and $CuSO_4$ treatments along component 1 (19.7%) (Figure S7A). When the proteins identified in the control and CNW treatments were processed separately, a clear separation of the CNW treatments and the control is noted along component 1 (12.3%) (Figure S7B). One-way ANOVA identified 15 differentially accumulated proteins

https://doi.org/10.1021/acs.est.1c00839
Environ. Sci. Technol. XXXX, XXX, XXX−XXX

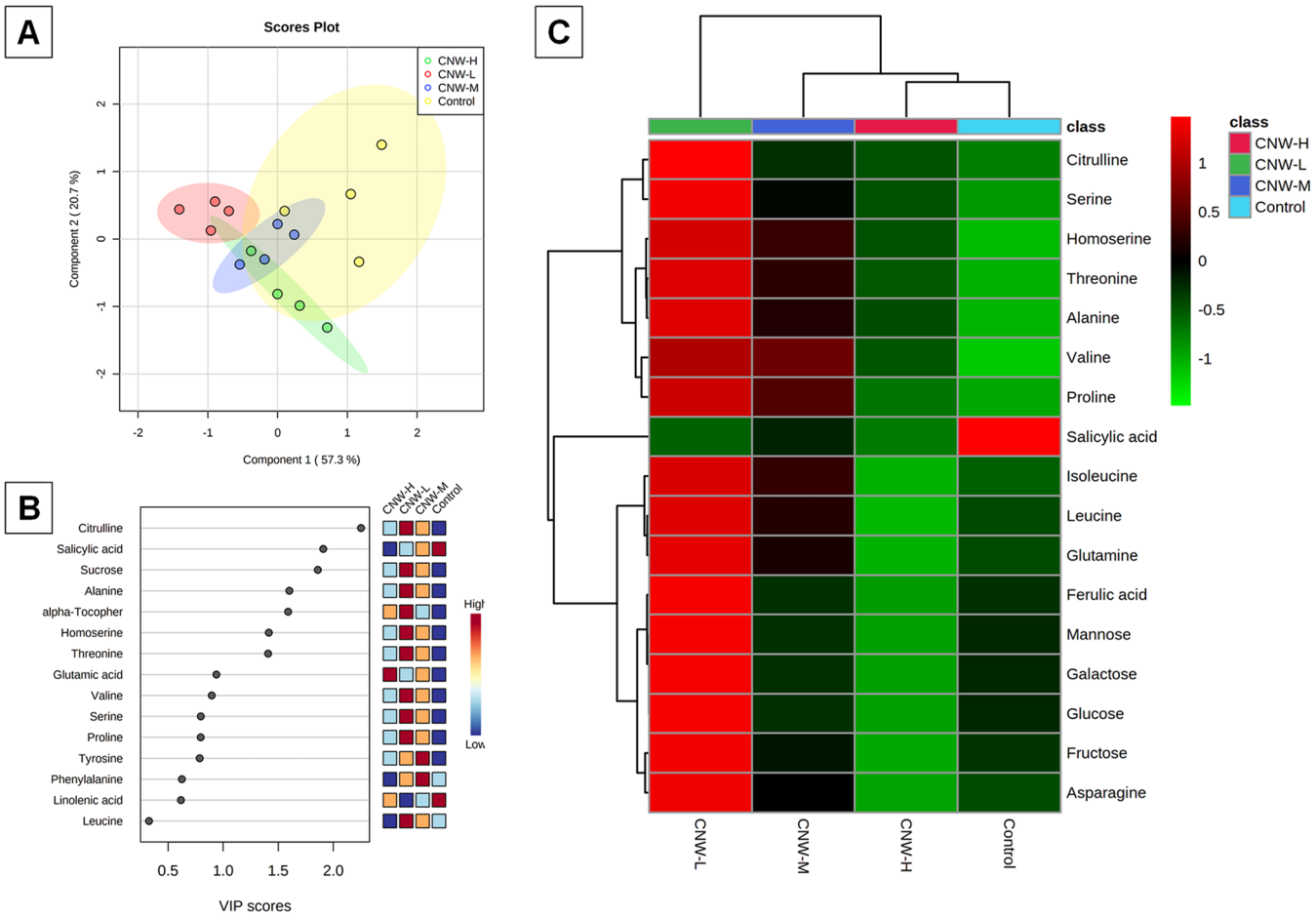

Figure 5. Targeted metabolomic analysis in the leaves of plants exposed to the control, CNW-L, CNW-M, and CNW-H treatments. (A) Heat map demonstrating the clusters with the abundance scale shown in the legend. (B) Abundance pattern of the differentially accumulated proteins in three clusters. (C) Gene ontology of the three clusters

(DAPs) between all treatments at $p \leq 0.05$ (Figure S8). However, a separate analysis of proteins from the CNW and control treatments was performed to identify CNW-specific protein abundance, which yielded 48 DAPs (Figure 4A, Table S8). Hierarchical clustering analysis grouped the DAPs into three distinct clusters based on abundance (Figure 4B, Table S9). Cluster 1 had 15 protein-groups that showed a higher abundance in CNW-L treatment compared to the control, CNW-M, and CNW-H. Although CNW-L did not show an overt physiological effect, the proteomics results suggest an activation of carbohydrate metabolism, lignin biosynthesis, and defense response in soybean plants, employing unique proteins that are not activated when Cu is present at a higher abundance. Cluster 2 consisted of seven protein-groups, which over-accumulated in all the CNW treatments but was most abundant in CNW-M treatment. It includes a cytosol protein, linoleate 9S-lipoxygenase, that is involved in fatty acid biosynthesis and a chloroplast protein, allene-oxide cyclase, which plays a key role in jasmonic acid biosynthesis. Thus, these proteins were involved in the defense response to cope with the high influx of Cu into the cells. Cluster 3 consisted of 26 protein groups that were significantly down-accumulated in CNW-L leaves, out of which 15 were down-accumulated in all the CNW treatments. These proteins were primarily involved in translation, mitochondrial L-ornithine transmembrane transport, chlorophyll biosynthesis, oxidoreductase activities, and glutaminyl-peptide cyclotransferase activity. In the same cluster, nine proteins were significantly overaccumulated in CNW-H and CNW-M treatments compared to the control and CNW-L, of which five were present in chloroplast stroma/thylakoid and participated in ATP binding and ribulose-1,5-bisphosphate carboxylase-oxygenase (RuBisCo) activation. Other cytosol proteins were associated with metal-ion binding, fructose-bisphosphate aldolase activity, and α-amylase activity involved in carbohydrate metabolism. Thus, the increase in A_{net} in CNW-H and CNW-M treatments can be explained by the over-accumulation of proteins involved in photosystem I and II reactions and energy production, thereby leading to an increase in shoot length. However, Kocide treatment modulated 41 proteins in the sobean leaves; 21 proteins were overaccumulated compared to the control, which were involved in glycogen and starch biosynthesis, phosphatidylcholine activity, GTP binding, and the structural constitution of ribosome for translation. The remaining 20 proteins showed a decreased abundance, which were related to carbohydrate metabolism, fatty acid β-oxidation, Fe-binding, and hydrogen peroxide catabolic processes, suggesting a response to oxidative stress.

Metabolomic Response in Soybean Plants Exposed to CNW. LC−MS/MS-based untargeted metabolomic analysis of the leaves across four treatment groups, including the control, CNW-H, Kocide, and $CuSO_4$, resulted in the detection of 3361 semipolar and nonpolar metabolites. As seen in the PLS-DA

https://doi.org/10.1021/acs.est.1c00839
Environ. Sci. Technol. XXXX, XXX, XXX−XXX

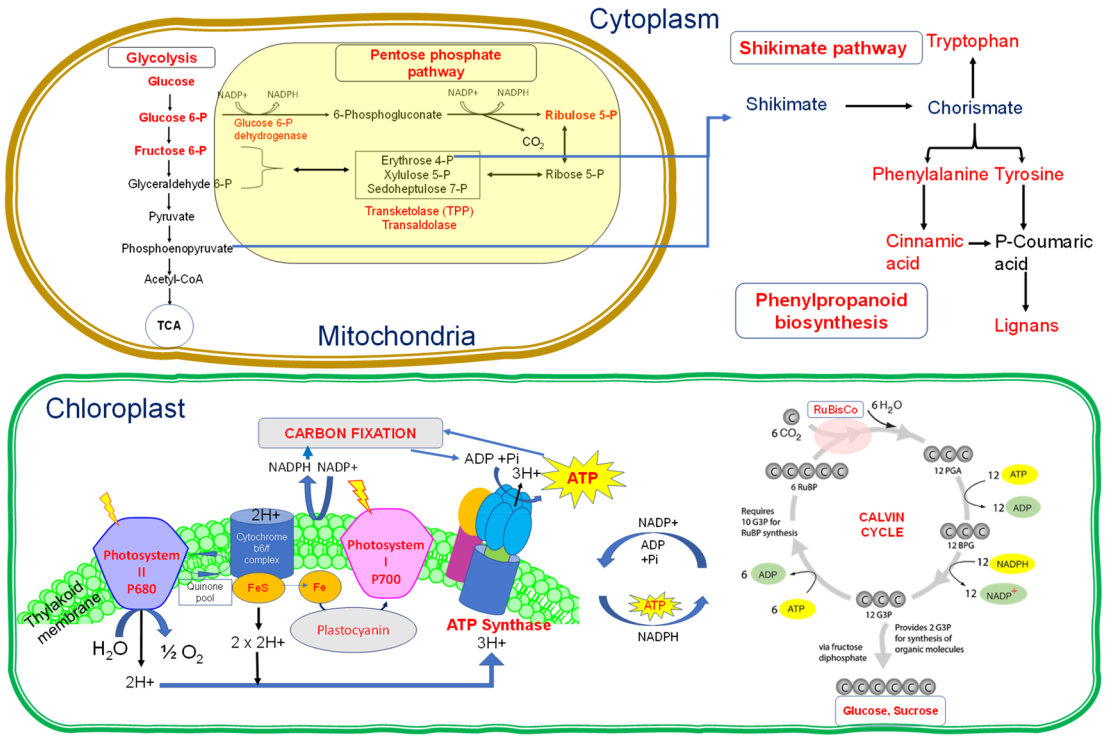

Figure 6. Schematic diagram of metabolic pathways in soybean plants activated in response to CNW treatments. Affected pathways and metabolites have been highlighted in red.

plot, Kocide was separated from the control and CNW-H along component 1 at 27.3%, and the hierarchical clustering based on the variable importance in projection (VIP) score illustrates the distinct metabolic features in the Kocide and $CuSO_4$ treatments (Figure S9A,B). However, there was no separation between the control and CNW-H treatments, and no significant features were noted. When the data analysis for metabolite concentrations in the control and CNW-H was performed excluding the other Cu treatments, the separation was clear along component 1, but only two features were significant at FDR $\leq$ 0.05. The combined targeted analysis of the polar metabolites identified 60 metabolites in the soybean leaves. The 2D-PLS-DA score plot suggests that the polar metabolites from Kocide were distinct from the control (Figure S10A). The top 15 important features were identified using a VIP score $\geq$1, which predominantly included amino acids and nucleotides, or their derivatives (Figure S10B). The soybean metabolites modulated in response to Kocide treatments was comparable to those of previous studies.[11,12,14] However, CNW-H treatment only showed an abundance of cyclic guanosine monophosphate compared to the control.

As distinct proteomic features were observed at different CNW doses (Figure 4), a deeper approach was undertaken further using targeted metabolomics by analyzing different groups of metabolites using independent LC−MS/MS methods. The PLS-DA score plot suggests a clear separation between CNW-L and other treatments (Figure 5, Figure S11), similar to the proteomic analysis. Seventeen metabolites were differentially accumulated in the leaves of CNW-L-treated plants compared to those of the control (Figure 5), which includes five sugars (glucose, sucrose, galactose, fructose, and mannose) and 11 amino acids (*Asn, Cit, Ser, Hse, Thr, Ala, Val, Pro, Ile, Leu,* and *Gln*). In CNW-M-treated plants, *Phe, Thr, Ile, Ala, Val,* and *Pro* were overaccumulated. However, most of the metabolite levels were lower in CNW-H leaves compared to the control and other CNW treatments (Figures S10B and S12), which could be due to a higher Cu concentration in the CNW-H shoots (Figure 2). Interestingly, all the Cu treatments including CNW-L, CNW-M, CNW-H, Kocide, and $CuSO_4$ resulted in a decrease in the concentration of salicylic acid. Salicylic acid is a phenolic compound that plays a crucial role in plants to alleviate stress due to heavy metals or other abiotic factors.[51] Compared to the control, in Kocide and $CuSO_4$ treatments, linolenic acid levels were also lowered, which is involved in jasmonic acid biosynthesis. Jasmonic acid is another signaling molecule involved in plant stress response to biotic and abiotic factors.[52] The amino acid *Glu,* which plays a central role in amino acid metabolism and glutathione cycle,[53] was significantly increased in Kocide- and $CuSO_4$-treated plants; although the CNW treatments also showed an increasing trend, they were not statistically significant (Figure S11).

Biological Pathways Activated in Response to CNW and Kocide. The mapping of the metabolites and proteins modulated by the CNW and Kocide treatments suggested that both treatments impacted aminoacyl-tRNA biosynthesis, amino acid metabolism, glyoxylate/dicarboxylate metabolism, nitrogen metabolism, phenylpropanoid biosynthesis, galactose metabolism, alkaloid biosynthesis, sulfur metabolism, sphingolipid metabolism, carbon fixation in photosynthetic process, starch/sucrose metabolism, glycolysis, fatty acid metabolism, and nucleotide metabolism (Tables S10 and S11).

The major biological processes that were affected by CNW treatment were photosynthesis and carbon fixation (Figure 6). At a lower CNW concentration, the enzymes associated with chlorophyll biosynthesis, oxidoreductase activity, and mitochondrial L-*Orn* transmembrane transport were less abundant; however, at a higher concentration (CNW-M and CNW-H), these enzymes located in chloroplast and mitochondrial

https://doi.org/10.1021/acs.est.1c00839
Environ. Sci. Technol. XXXX, XXX, XXX−XXX

membrane were activated resulting in increased RuBisCo activity, ATP-binding, and transmembrane transport. Plastocyanin is a Cu-containing photosynthetic enzyme that mediates the transport of electron in thylakoids from stacked grana where photosystem II takes place to unstacked regions that harbor photosystem I.[54] Hence, increased Cu availability improves the photosynthetic process in CNW-treated plants, at a higher concentration. This also corroborates with the elemental composition that shows an increased Fe concentration in CNW-M and CNW-H shoots, which is also involved in the photosynthetic process. CNW-H treatment also yielded an increase in fructose-bisphosphate aldolase, which participates in glycolysis to convert fructose 1,6 bisphosphate to glyceraldehyde-3-phosphate. α-Amylase that catalyzes the hydrolysis of α-1,4-glucosidic bonds of glycogen, starch, and related polysaccharides was also accumulated significantly more in the CNW-H-treated plants, suggesting an increase in energy production (Table S10). The hexose levels were however lower in the leaves from CNW-H treatments, compared to the control and other Cu treatments, which could be explained by the utilization of these metabolites for energy production, resulting in an increased shoot length of the CNW-H-treated plants (Figure S3). Previous foliar exposure studies in cucumber plants showed that high doses of Kocide (2.1 mg Cu/plant) perturbed sucrose and sugar metabolism and carbon fixation.[18]

An increase in the accumulation of the hexose sugars (sucrose, glucose, fructose, mannose, galactose) in the leaves from CNW-L- and CNW-M-treated plants signify an increase in the photosynthetic activity; however, the gas-exchange activities did not show any significant effects at the lower dose. This also corroborates the proteomic findings, where sucrose synthase, α-galactosidase, and glucan endo-1,3-β-glucosidase were overaccumulated in CNW-L and CNW-M, demonstrating an activation of sugar metabolism. NADH dehydrogenase (ubiquinone) 4Fe-4S protein complex showed enhanced levels in CNW-L-treated plants. This protein participates in electron transfer from NADH to the respiratory chain.[55] Another enzyme, 6-phosphogluconate dehydrogenase, was also overaccumulated in CNW-L and CNW-M leaves. 6-Phosphogluconate dehydrogenase catalyzes the decarboxylating reduction of 6-phosphogluconate into ribulose 5-phosphate in the presence of nicotinamide adenine dinucleotide phosphate (NADP) in the pentose-phosphate pathway, which is a parallel pathway to glycolysis. CNW-M also activated fatty acid biosynthesis as noted by the increased levels of lipoxygenase and allene-oxide cyclase; however, the gas-exchange activities did not show any significant effects at the lower dose.

In terms of stress response, the γ-glutaminyl-peptide cyclotransferase level was enhanced in CNW-M and CNW-H leaves, whereas it was significantly less abundant in the lower exposure dose. This enzyme converts *Gln* and *N*-terminal glutamyl residues in peptides to 5-oxoproline and 5-oxoproline residues. This was also reflected in the metabolomic analysis, where *Gln* was significantly decreased in all the treatments with respect to the control, except CNW-L. CNW-M and CNW-H resulted in increased levels of cinnamyl-alcohol dehydrogenase, which is directly involved in lignin biosynthesis *via* the phenylpropanoid pathway. However, salicylic acid, an early product of the shikimate pathway was decreased in all Cu treatments, suggesting an active stress response by the soybean plants against Cu treatments. The activation of the phenylpropanoid pathways in the CNW and Kocide treatments corroborates the lignin accumulation results, which showed high levels after 16 d of exposure in all the treatments, except CNW-L (Figure S4). In CNW-L leaves, the increased level of ferulic acid formed as a product of phenylpropanoid pathway, was responsible for alleviating oxidative stress.

Although stress response pathways were activated by CNWs at the highest concentration, Kocide treatment induced more stress response pathways and modulated amino acid synthesis involved in various metabolic processes. Only Kocide treatment resulted in an increased accumulation of antioxidant compounds including *Glu*, α-tocopherol, and amino acid precursors for the phenylpropanoid pathway (*Phe*, *Tyr*, and *Trp*). In addition, *Met* was exclusively overaccumulated in Kocide-exposed plants, resulting in the activation of *Cys*−*Met* metabolism. These S-containing amino acids are precursors to various antioxidant metabolites such as glutathione, phytochelatins, S-adenosylmethionine, ethylene, and polyamines.[56] In addition, two proteins, S-adenosylmethionine synthase and methionine synthase, were also overaccumulated in Kocide-treated plants. The activation of stress response in the plants upon exposure to Kocide plants corroborates previous studies reporting the impact on oxidative stress and amino acid metabolism in corn, lettuce, cucumber, and spinach plants.[11,12,18,57]

Thus, from the integration of proteomic and metabolomic fingerprints, we conclude that CNW at a low concentration activates the sugar and fatty acid metabolism but only activates the pathways involved in photosynthesis and energy metabolism at higher concentrations (Figure 6). Although Kocide also activates the sugar metabolism and energy production, it activates a greater number of oxidative stress pathways, which could be due to the rapid availability of Cu during the early exposure period in contrast to CNW treatments, where Cu translocation is slower. It was apparent from the Cu accumulation studies that CNW exposure resulted in a slow release of Cu to the aerial and root tissues, compared to Kocide and $CuSO_4$ treatments. This also results in differential response in the metabolic processes of the soybean plants.

This study highlights the use and integration of proteomics and multiplatform metabolomics to elucidate the molecular mechanisms leading to physiological and metabolic alterations in plants in response to engineered nanomaterials. This study for the first time revealed the proteins and metabolites in soybean plants associated with the response to CNW in comparison to Kocide by utilizing omic approaches. The integration of discovery proteomics with metabolomics identified photosynthesis, carbohydrate metabolism, amino acid metabolism, phenylpropanoid biosynthesis, and fatty acid metabolism as the major metabolic pathways that were affected by CNW and Kocide exposure. Thus, a holistic understanding of the underlying molecular mechanisms and the factors influencing the uptake and biological response can result in a safer application of copper-based nanopesticides in the future.

■ ASSOCIATED CONTENT

Supporting Information

The Supporting Information is available free of charge at https://pubs.acs.org/doi/10.1021/acs.est.1c00839.

Methods of gas-exchange activities, proteomic analysis, and metabolomic analysis, tables of list of targeted metabolites analyzed by LC−MS/MS, fresh biomass of soybean root and shoot, copper translocation from exposed shoot tissues to unexposed shoot and root tissues, elemental contents in the plant tissues, and

https://doi.org/10.1021/acs.est.1c00839
Environ. Sci. Technol. XXXX, XXX, XXX−XXX

soybean metabolic pathways activated by CNW exposure and Kocide exposure, and figures of experimental set-up for foliar spray exposure of soybean plants to Cu treatments, average hydrodynamic diameter and ζ-potential of CNW suspensions, root and shoot lengths, lignin content, proteins identified in leaves of soybean plants, multiscatter plots, two dimensional-PLS-DA score plots and hierarchical clustering analysis of identified proteins, leaf metabolites identified by untargeted and targeted metabolomic analysis, and differentially accumulated metabolites (PDF)

Tables of list of identified proteins in the leaves of soybean plants, gene ontology of unique proteins identified in all Cu treatments and CNW treatments, list of identified and differentially accumulated proteins in the leaves of soybean plants, and list of hierarchical clusters of proteins in the leaves of soybean plants (XLSX)

AUTHOR INFORMATION

Corresponding Author

Arturo A. Keller − *Bren School of Environmental Science and Management, University of California, Santa Barbara, California 93106, United States; University of California Center for Environmental Implications of Nanotechnology (UC CEIN), Santa Barbara, California 93106, United States;* orcid.org/0000-0002-7638-662X; Phone: 805-893-7548; Email: keller@bren.ucsb.edu; Fax: 805-893-7612

Authors

Sanghamitra Majumdar − *Bren School of Environmental Science and Management, University of California, Santa Barbara, California 93106, United States; University of California Center for Environmental Implications of Nanotechnology (UC CEIN), Santa Barbara, California 93106, United States*

Randall W. Long − *Ecology, Evolution, and Marine Biology, University of California, Santa Barbara, California 93106, United States*

Jay S. Kirkwood − *Institute for Integrative Genome Biology, Department of Botany and Plant Sciences, University of California, Riverside, California 92521, United States*

Anastasiia S. Minakova − *Bren School of Environmental Science and Management, University of California, Santa Barbara, California 93106, United States*

Complete contact information is available at: https://pubs.acs.org/10.1021/acs.est.1c00839

Notes

The authors declare no competing financial interest.

ACKNOWLEDGMENTS

This material is based upon work supported by the National Science Foundation under Grant No. **1901515**. The authors would like to thank Dr. Yu Chen and the Molecular Instrumentation Center, UCLA Department of Chemistry and Biochemistry for desalting and running the proteomic samples on LC−MS/MS. The authors would like to thank the UC Riverside Metabolomics Core for providing instrumentation for metabolomics analysis. Any opinions, findings, and conclusions or recommendations expressed in this material are those of the author(s) and do not necessarily reflect the views of the National Science Foundation.

REFERENCES

(1) Kah, M.; Tufenkji, N.; White, J. C. Nano-enabled strategies to enhance crop nutrition and protection. *Nat. Nanotechnol.* **2019**, *14* (6), 532−540.

(2) Iavicoli, I.; Leso, V.; Beezhold, D. H.; Shvedova, A. A. Nanotechnology in agriculture: Opportunities, toxicological implications, and occupational risks. *Toxicol. Appl. Pharmacol.* **2017**, *329*, 96−111.

(3) Majumdar, S.; Keller, A. A. Omics to address the opportunities and challenges of nanotechnology in agriculture. *Crit. Rev. Environ. Sci. Technol.* **2020**, 1−42.

(4) Marschner, H. Preface to Second Edition. In *Marschner's Mineral Nutrition of Higher Plants*, Third ed.;Marschner, P., Ed.; Academic Press:: San Diego, CA, 2012; p ix.

(5) Ravet, K.; Pilon, M. Copper and iron homeostasis in plants: the challenges of oxidative stress. *Antioxid. Redox Signaling* **2013**, *19* (9), 919−932.

(6) Yruela, I. Copper in plants. *Braz. J. Plant Physiol.* **2005**, *17*, 145−156.

(7) *Reregistration Eligibility Decision (RED) for Coppers*; U.S. Environmental Protection Agency, Pesticides and Toxic Substances, Office of Pesticide Programs, Eds.; U.S. Government Printing Office: Washington, DC, 2009.

(8) Keller, A. A.; Adeleye, A. S.; Conway, J. R.; Garner, K. L.; Zhao, L.; Cherr, G. N.; Hong, J.; Gardea-Torresdey, J. L.; Godwin, H. A.; Hanna, S.; Ji, Z.; Kaweeteerawat, C.; Lin, S.; Lenihan, H. S.; Miller, R. J.; Nel, A. E.; Peralta-Videa, J. R.; Walker, S. L.; Taylor, A. A.; Torres-Duarte, C.; Zink, J. I.; Zuverza-Mena, N. Comparative environmental fate and toxicity of copper nanomaterials. *NanoImpact* **2017**, *7*, 28−40.

(9) Tamez, C.; Hernandez-Molina, M.; Hernandez-Viezcas, J. A.; Gardea-Torresdey, J. L. Uptake, transport, and effects of nano-copper exposure in zucchini (Cucurbita pepo). *Sci. Total Environ.* **2019**, *665*, 100−106.

(10) Hong, J.; Rico, C. M.; Zhao, L.; Adeleye, A. S.; Keller, A. A.; Peralta-Videa, J. R.; Gardea-Torresdey, J. L. Toxic effects of copper-based nanoparticles or compounds to lettuce (Lactuca sativa) and alfalfa (Medicago sativa). *Environmental Science: Processes & Impacts* **2015**, *17* (1), 177−185.

(11) Zhao, L.; Ortiz, C.; Adeleye, A. S.; Hu, Q.; Zhou, H.; Huang, Y.; Keller, A. A. Metabolomics to Detect Response of Lettuce (Lactuca sativa) to Cu(OH)2 Nanopesticides: Oxidative Stress Response and Detoxification Mechanisms. *Environ. Sci. Technol.* **2016**, *50* (17), 9697−9707.

(12) Zhao, L.; Huang, Y.; Keller, A. A. Comparative Metabolic Response between Cucumber (Cucumis sativus) and Corn (Zea mays) to a Cu(OH)2 Nanopesticide. *J. Agric. Food Chem.* **2018**, *66* (26), 6628−6636.

(13) Zhao, L.; Huang, Y.; Hannah-Bick, C.; Fulton, A. N.; Keller, A. A. Application of metabolomics to assess the impact of Cu(OH)2 nanopesticide on the nutritional value of lettuce (Lactuca sativa): Enhanced Cu intake and reduced antioxidants. *NanoImpact* **2016**, *3*−*4*, 58−66.

(14) Zhao, L.; Huang, Y.; Adeleye, A. S.; Keller, A. A. Metabolomics Reveals $Cu(OH)_2$ Nanopesticide-Activated Anti-oxidative Pathways and Decreased Beneficial Antioxidants in Spinach Leaves. *Environ. Sci. Technol.* **2017**, *51* (17), 10184−10194.

(15) Zhao, L.; Hu, Q.; Huang, Y.; Fulton, A. N.; Hannah-Bick, C.; Adeleye, A. S.; Keller, A. A. Activation of antioxidant and detoxification gene expression in cucumber plants exposed to a Cu(OH)2 nanopesticide. *Environ. Sci.: Nano* **2017**, *4* (8), 1750−1760.

(16) Valdes, C.; Cota-Ruiz, K.; Flores, K.; Ye, Y.; Hernandez-Viezcas, J. A.; Gardea-Torresdey, J. L. Antioxidant and defense genetic expressions in corn at early-developmental stage are differentially modulated by copper form exposure (nano, bulk, ionic): Nutrient and physiological effects. *Ecotoxicol. Environ. Saf.* **2020**, *206*, 111197.

(17) Zhao, L.; Huang, Y.; Zhou, H.; Adeleye, A. S.; Wang, H.; Ortiz, C.; Mazer, S. J.; Keller, A. A. GC-TOF-MS based metabolomics and ICP-MS based metallomics of cucumber (Cucumis sativus) fruits reveal alteration of metabolites profile and biological pathway disruption induced by nano copper. *Environ. Sci.: Nano* **2016**, *3* (5), 1114−1123.
(18) Zhao, L.; Huang, Y.; Paglia, K.; Vaniya, A.; Wancewicz, B.; Keller, A. A. Metabolomics Reveals the Molecular Mechanisms of Copper Induced Cucumber Leaf (Cucumis sativus) Senescence. *Environ. Sci. Technol.* **2018**, *52* (12), 7092−7100.
(19) Ma, C.; Borgatta, J.; Hudson, B. G.; Tamijani, A. A.; De La Torre-Roche, R.; Zuverza-Mena, N.; Shen, Y.; Elmer, W.; Xing, B.; Mason, S. E.; Hamers, R. J.; White, J. C. Advanced material modulation of nutritional and phytohormone status alleviates damage from soybean sudden death syndrome. *Nat. Nanotechnol.* **2020**, *15* (12), 1033−1042.
(20) Elmer, W.; De La Torre-Roche, R.; Pagano, L.; Majumdar, S.; Zuverza-Mena, N.; Dimkpa, C.; Gardea-Torresdey, J.; White, J. C. Effect of Metalloid and Metal Oxide Nanoparticles on Fusarium Wilt of Watermelon. *Plant Dis.* **2018**, *102* (7), 1394−1401.
(21) Borgatta, J.; Ma, C.; Hudson-Smith, N.; Elmer, W.; Plaza Pérez, C. D.; De La Torre-Roche, R.; Zuverza-Mena, N.; Haynes, C. L.; White, J. C.; Hamers, R. J. Copper Based Nanomaterials Suppress Root Fungal Disease in Watermelon (Citrullus lanatus): Role of Particle Morphology, Composition and Dissolution Behavior. *ACS Sustainable Chem. Eng.* **2018**, *6* (11), 14847−14856.
(22) Cota-Ruiz, K.; Ye, Y.; Valdes, C.; Deng, C.; Wang, Y.; Hernández-Viezcas, J. A.; Duarte-Gardea, M.; Gardea-Torresdey, J. L. Copper nanowires as nanofertilizers for alfalfa plants: Understanding nano-bio systems interactions from microbial genomics, plant molecular responses and spectroscopic studies. *Sci. Total Environ.* **2020**, *742*, 140572.
(23) Kim, E.; Hwang, S.; Lee, I. SoyNet: a database of co-functional networks for soybean Glycine max. *Nucleic Acids Res.* **2017**, *45* (D1), D1082−D1089.
(24) Moreira-Vilar, F. C.; Siqueira-Soares, R. d. C.; Finger-Teixeira, A.; Oliveira, D. M. d.; Ferro, A. P.; da Rocha, G. J.; Ferrarese, M. d. L. L.; dos Santos, W. D.; Ferrarese-Filho, O. The Acetyl Bromide Method Is Faster, Simpler and Presents Best Recovery of Lignin in Different Herbaceous Tissues than Klason and Thioglycolic Acid Methods. *PLoS One* **2014**, *9* (10), e110000.
(25) Majumdar, S.; Almeida, I. C.; Arigi, E. A.; Choi, H.; VerBerkmoes, N. C.; Trujillo-Reyes, J.; Flores-Margez, J. P.; White, J. C.; Peralta-Videa, J. R.; Gardea-Torresdey, J. L. Environmental Effects of Nanoceria on Seed Production of Common Bean (Phaseolus vulgaris): A Proteomic Analysis. *Environ. Sci. Technol.* **2015**, *49* (22), 13283−13293.
(26) Kaiser, P.; Wohlschlegel, J. Identification of Ubiquitination Sites and Determination of Ubiquitin-Chain Architectures by Mass Spectrometry. In *Methods in Enzymology*; Academic Press, 2005; Vol. *399*, pp 266−277.
(27) Majumdar, S.; Pagano, L.; Wohlschlegel, J. A.; Villani, M.; Zappettini, A.; White, J. C.; Keller, A. A. Proteomic, gene and metabolite characterization reveal the uptake and toxicity mechanisms of cadmium sulfide quantum dots in soybean plants. *Environ. Sci.: Nano* **2019**, *6* (10), 3010−3026.
(28) Perez-Riverol, Y.; Csordas, A.; Bai, J.; Bernal-Llinares, M.; Hewapathirana, S.; Kundu, D. J.; Inuganti, A.; Griss, J.; Mayer, G.; Eisenacher, M.; Pérez, E.; Uszkoreit, J.; Pfeuffer, J.; Sachsenberg, T.; Yilmaz, S.; Tiwary, S.; Cox, J.; Audain, E.; Walzer, M.; Jarnuczak, A. F.; Ternent, T.; Brazma, A.; Vizcaíno, J. A. The PRIDE database and related tools and resources in 2019: improving support for quantification data. *Nucleic Acids Res.* **2019**, *47* (D1), D442−D450.
(29) Cox, J.; Mann, M. MaxQuant enables high peptide identification rates, individualized p.p.b.-range mass accuracies and proteome-wide protein quantification. *Nat. Biotechnol.* **2008**, *26* (12), 1367.
(30) Tyanova, S.; Temu, T.; Sinitcyn, P.; Carlson, A.; Hein, M. Y.; Geiger, T.; Mann, M.; Cox, J. The Perseus computational platform for comprehensive analysis of (prote)omics data. *Nat. Methods* **2016**, *13*, 731.
(31) The UniProt Consortium. UniProt: a worldwide hub of protein knowledge. *Nucleic Acids Res.* **2018**, *47* (D1), D506−D515.
(32) Morishima, K.; Tanabe, M.; Furumichi, M.; Kanehisa, M.; Sato, Y. New approach for understanding genome variations in KEGG. *Nucleic Acids Res.* **2019**, *47* (D1), D590−D595.
(33) Rothman, J. A.; Leger, L.; Kirkwood, J. S.; McFrederick, Q. S. Cadmium and selenate exposure affects the honey bee microbiome and metabolome, and bee-associated bacteria show potential for bioaccumulation. *Appl. Environ. Microbiol.* **2019**, *85* (21), e01411.
(34) Vliet, S. M. F.; Dasgupta, S.; Sparks, N. R. L.; Kirkwood, J. S.; Vollaro, A.; Hur, M.; Zur Nieden, N. I.; Volz, D. C. Maternal-to-zygotic transition as a potential target for niclosamide during early embryogenesis. *Toxicol. Appl. Pharmacol.* **2019**, *380*, 114699.
(35) Huang, Y.; Adeleye, A. S.; Zhao, L.; Minakova, A. S.; Anumol, T.; Keller, A. A. Antioxidant response of cucumber (Cucumis sativus) exposed to nano copper pesticide: Quantitative determination via LC-MS/MS. *Food Chem.* **2019**, *270*, 47−52.
(36) Huang, Y.; Li, W.; Minakova, A. S.; Anumol, T.; Keller, A. A. Quantitative analysis of changes in amino acids levels for cucumber (Cucumis sativus) exposed to nano copper. *NanoImpact* **2018**, *12*, 9−17.
(37) Dunn, W. B; Broadhurst, D.; Begley, P.; Zelena, E.; Francis-McIntyre, S.; Anderson, N.; Brown, M.; Knowles, J. D; Halsall, A.; Haselden, J. N; Nicholls, A. W; Wilson, I. D; Kell, D. B; Goodacre, R. Procedures for large-scale metabolic profiling of serum and plasma using gas chromatography and liquid chromatography coupled to mass spectrometry. *Nat. Protoc.* **2011**, *6* (7), 1060−1083.
(38) Barupal, D. K.; Fan, S.; Wancewicz, B.; Cajka, T.; Sa, M.; Showalter, M. R.; Baillie, R.; Tenenbaum, J. D.; Louie, G.; Kaddurah-Daouk, R.; Fiehn, O. Generation and quality control of lipidomics data for the alzheimer's disease neuroimaging initiative cohort. *Sci. Data* **2018**, *5* (1), 180263.
(39) Broeckling, C. D.; Afsar, F. A.; Neumann, S.; Ben-Hur, A.; Prenni, J. E. RAMClust: a novel feature clustering method enables spectral-matching-based annotation for metabolomics data. *Anal. Chem.* **2014**, *86* (14), 6812−7.
(40) Sumner, L. W.; Amberg, A.; Barrett, D.; Beale, M. H.; Beger, R.; Daykin, C. A.; Fan, T. W.; Fiehn, O.; Goodacre, R.; Griffin, J. L.; Hankemeier, T.; Hardy, N.; Harnly, J.; Higashi, R.; Kopka, J.; Lane, A. N.; Lindon, J. C.; Marriott, P.; Nicholls, A. W.; Reily, M. D.; Thaden, J. J.; Viant, M. R. Proposed minimum reporting standards for chemical analysis Chemical Analysis Working Group (CAWG) Metabolomics Standards Initiative (MSI). *Metabolomics* **2007**, *3* (3), 211−221.
(41) Schymanski, E. L.; Jeon, J.; Gulde, R.; Fenner, K.; Ruff, M.; Singer, H. P.; Hollender, J. Identifying small molecules via high resolution mass spectrometry: communicating confidence. *Environ. Sci. Technol.* **2014**, *48* (4), 2097−8.
(42) MacLean, B.; Tomazela, D. M.; Shulman, N.; Chambers, M.; Finney, G. L.; Frewen, B.; Kern, R.; Tabb, D. L.; Liebler, D. C.; MacCoss, M. J. Skyline: an open source document editor for creating and analyzing targeted proteomics experiments. *Bioinformatics* **2010**, *26* (7), 966−8.
(43) Chong, J.; Soufan, O.; Li, C.; Caraus, I.; Li, S.; Bourque, G.; Wishart, D. S.; Xia, J. MetaboAnalyst 4.0: towards more transparent and integrative metabolomics analysis. *Nucleic Acids Res.* **2018**, *46* (W1), W486−W494.
(44) Szklarczyk, D.; Morris, J. H.; Cook, H.; Kuhn, M.; Wyder, S.; Simonovic, M.; Santos, A.; Doncheva, N. T.; Roth, A.; Bork, P.; Jensen, L. J.; von Mering, C. The STRING database in 2017: quality-controlled protein-protein association networks, made broadly accessible. *Nucleic Acids Res.* **2017**, *45* (D1), D362−D368.
(45) Adeleye, A. S.; Conway, J. R.; Perez, T.; Rutten, P.; Keller, A. A. Influence of Extracellular Polymeric Substances on the Long-Term Fate, Dissolution, and Speciation of Copper-Based Nanoparticles. *Environ. Sci. Technol.* **2014**, *48* (21), 12561−12568.
(46) Amberger, A.; Gutser, R.; Wunsch, A. Iron chlorosis induced by high copper and manganese supply. *J. Plant Nutr.* **1982**, *5* (4−7), 715−720.

https://doi.org/10.1021/acs.est.1c00839
Environ. Sci. Technol. XXXX, XXX, XXX−XXX

(47) Keller, A. A.; Huang, Y.; Nelson, J. Detection of nanoparticles in edible plant tissues exposed to nano-copper using single-particle ICP-MS. *J. Nanopart. Res.* **2018**, *20* (4), 101.
(48) Lin, C.-C.; Chen, L.-M.; Liu, Z.-H. Rapid effect of copper on lignin biosynthesis in soybean roots. *Plant Sci.* **2005**, *168* (3), 855−861.
(49) Rawat, S.; Pullagurala, V. L. R.; Hernandez-Molina, M.; Sun, Y.; Niu, G.; Hernandez-Viezcas, J. A.; Peralta-Videa, J. R.; Gardea-Torresdey, J. L. Impacts of copper oxide nanoparticles on bell pepper (Capsicum annum L.) plants: a full life cycle study. *Environ. Sci.: Nano* **2018**, *5* (1), 83−95.
(50) Ye, S.; Von Delft, F.; Brooun, A.; Knuth, M. W.; Swanson, R. V.; McRee, D. E. The crystal structure of shikimate dehydrogenase (AroE) reveals a unique NADPH binding mode. *J. Bacteriol.* **2003**, *185* (14), 4144−4151.
(51) Janda, T.; Gondor, O. K.; Yordanova, R.; Szalai, G.; Pál, M. Salicylic acid and photosynthesis: signalling and effects. *Acta Physiol. Plant.* **2014**, *36* (10), 2537−2546.
(52) Wang, J.; Song, L.; Gong, X.; Xu, J.; Li, M. Functions of Jasmonic Acid in Plant Regulation and Response to Abiotic Stress. *Int. J. Mol. Sci.* **2020**, *21* (4), 1446.
(53) Forde, B. G.; Lea, P. J. Glutamate in plants: metabolism, regulation, and signalling. *J. Exp. Bot.* **2007**, *58* (9), 2339−2358.
(54) Höhner, R.; Pribil, M.; Herbstová, M.; Lopez, L. S.; Kunz, H.-H.; Li, M.; Wood, M.; Svoboda, V.; Puthiyaveetil, S.; Leister, D.; Kirchhoff, H. Plastocyanin is the long-range electron carrier between photosystem II and photosystem I in plants. *Proc. Natl. Acad. Sci. U. S. A.* **2020**, *117* (26), 15354.
(55) Wydro, M. M.; Sharma, P.; Foster, J. M.; Bych, K.; Meyer, E. H.; Balk, J. The evolutionarily conserved iron-sulfur protein INDH is required for complex I assembly and mitochondrial translation in *Arabidopsis*. *Plant Cell* **2013**, *25* (10), 4014−4027.
(56) Nikiforova, V.; Kempa, S.; Zeh, M.; Maimann, S.; Kreft, O.; Casazza, A. P.; Riedel, K.; Tauberger, E.; Hoefgen, R.; Hesse, H. Engineering of cysteine and methionine biosynthesis in potato. *Amino Acids* **2002**, *22* (3), 259−278.
(57) Zhao, L.; Huang, Y.; Hu, J.; Zhou, H.; Adeleye, A. S.; Keller, A. A. 1H NMR and GC-MS Based Metabolomics Reveal Defense and Detoxification Mechanism of Cucumber Plant under Nano-Cu Stress. *Environ. Sci. Technol.* **2016**, *50* (4), 2000−2010.

NOTE ADDED AFTER ASAP PUBLICATION

Due to a production error, this paper was published ASAP on July 9, 2021, with Figure 4 and 5 graphics transposed. The corrected version was reposted on July 12, 2021.

https://doi.org/10.1021/acs.est.1c00839
Environ. Sci. Technol. XXXX, XXX, XXX−XXX